RESEARCH ARTICLE

Frontiers of Biogeography
the scientific journal of
the International Biogeography Society

Energy use of modern terrestrial large mammal communities mirrors Late Pleistocene megafaunal extinctions

Benjamin E. Carter[1*] and John Alroy[1]

[1]School of Natural Sciences, Macquarie University, Sydney, NSW 2109, Australia.

*Correspondence: Benjamin E. Carter, benjamin.carter1@hdr.mq.edu.au

Abstract

Globally, large mammals are in decline. Biological traits including low population densities and longer generation times make them particularly susceptible. Their losses can have wide-ranging ecological consequences, including dramatic reductions in total heterotrophic energy use. To determine the key drivers of variation in energy use, we calculated daily rates of energy flow across the globe for 241 ecological communities, encompassing 441 large mammal species, using camera trap inventories. These were scaled up from individual metabolic rates and compared with various climate, anthropogenic, geographic, and species richness variables using three analytical methods: model selection, spatial autoregression, and a multiple regression method that completely removes multicollinearity known as least-squares orthogonalization. Community energy use is significantly lower in the Neotropics and Australasia than in the Afrotropics and Eurasia. This pattern mirrors the spatial distribution of megafaunal extinction intensity during the Late Pleistocene. Rates not being greatly reduced in the Nearctic is a notable exception to this pattern, and is likely due to the high abundances of certain species not present in the other highly-impacted realms. There are also strong negative correlations between community per-gram rates of energy flow and species richness, indicating that megafauna persist mainly in more speciose communities. The strong geographic differences that dominate energy use patterns indicate that past mammal extinctions are the ultimate cause of modern energetic variation in large mammal communities. If so, then ongoing losses of large mammals will greatly impact community and ecosystem functioning.

Highlights

- Large mammals are essential in maintaining community and ecosystem functioning as they dictate the total amount of heterotrophic energy use in natural systems.
- We quantified global variation in energy use of modern large mammal communities using 241 ecological camera trap inventories.
- The spatial distribution of modern-day energy use patterns largely matches the variation seen in megafaunal extinction intensity across the Late Pleistocene, with more greatly impacted regions exhibiting consistently lower rates of community energy flow.
- The apparent lack of recovery in certain regions suggests that current large mammal extinctions will have long-lasting impacts on community energetics around the globe.

Keywords: camera traps, community energy use, macroecology, megafauna, metabolic rate, large mammals, Pleistocene extinctions

Introduction

The Earth is in the midst of an ongoing biodiversity crisis with rapid and unprecedented rates of species declines (Barnosky et al. 2011, Dirzo et al. 2014). Conservative estimates suggest that vertebrate species losses alone are up to a hundred times faster than the usual background extinction rate (Ceballos et al. 2015). Larger species are particularly vulnerable, primarily due to their lower population densities, reduced reproductive rates, and increased generation times (Brook and Bowman 2005). Anthropogenic impacts such as hunting, habitat destruction, and land use disproportionately impact larger organisms (Ripple et al. 2019) and are further exacerbated by these traits, leading to even greater extinction risk for mammals weighing over three kilograms (Cardillo et al. 2005).

e-ISSN: 1948-6596 https://escholarship.org/uc/fb doi:10.21425/F5FBG62724

As ecosystem engineers, megafauna have outsized effects on communities. Their reduction or extirpation can have considerable cascading effects on trophic interactions, overall ecosystem function, and biogeochemical cycles (Estes et al. 2011, Smith et al. 2016, Forbes et al. 2019). Indeed, global simulations predict continued losses of large organisms will lead to significant reductions in global ecosystem productivity, heterotrophic biomass, and energy use (Enquist et al. 2020).

Energy is especially important as it is the fundamental property of natural systems (Odum 1968). Furthermore, the amount of total energy flux of an ecosystem is highly correlated with the maximum size of individual organisms; heterotrophic energy flux is predicted to scale superlinearly with total heterotrophic biomass by a power of 1.25 (Enquist et al. 2020). Since community and ecosystem energy use is ultimately dictated by individual metabolism (Enquist et al. 2003, Brown et al. 2004, Marquet et al. 2005, Schramski et al. 2015), the disproportionate amount of energy taken up by large organisms in ecosystems is a direct result of their higher total metabolic rates (McNab 2008), a consequence of their greater energy requirements. As large mammal species are most at risk from extinction, and as their losses have the greatest effects on energy use, it is imperative to understand how energy usage of large mammal communities varies around the world. This knowledge can be used to forecast future ecosystem energetics and prioritize conservation efforts.

Here, daily rates of energy flow of terrestrial large mammal communities are calculated for 241 ecological camera trap inventories across the globe. Community energy flow is here defined as the total metabolic output of all terrestrial mammalian species in an ecological community with an average body mass of 1 kg or more. As with previous studies (Ernest 2005, Barneche et al. 2014, Carter and Alroy 2022), rates of community energy flow are scaled up from individual metabolic rates and compared to factors including biogeography, species richness, and various climate and anthropogenic variables.

Energy use in large mammal communities should vary biogeographically, as seen with individual metabolic rates (Lovegrove 2000). The primary driver of biogeographic patterns is expected to be the current geographic distribution of the largest mammal species. Realms with a greater number of extant megafaunal species (e.g. the Afrotropics and Indomalaya) are predicted to have higher rates of community energy flow because very large species have high total metabolisms (McNab 2008, Enquist et al. 2020). Notably, megafaunal species were previously widespread across all geographic realms before many went extinct during the Late Pleistocene, severely altering continental body size distributions around the world (Sandom et al. 2014, Smith et al. 2018).

Relationships with species richness are predicted to be mixed. More speciose communities should have higher rates of community energy flow, especially those with a greater number or abundance of larger species. However, while larger mammals have higher whole-organism metabolic rates (McNab 2008), they have lower mass-specific rates, i.e., their overall metabolic intensity, or rate in which energy and resources are processed, is reduced (Hulbert and Else 2000, Savage et al. 2007). This negative relationship should be replicated on the community level. Communities with lower total rates of energy flow should have higher per-gram rates and vice versa. Therefore, less diverse communities with predicted low rates of total energy flow should have high per-gram rates, particularly if the lack of large species in a community is compensated by increased abundances of smaller species with high mass-specific metabolisms (Ernest and Brown 2001).

Lastly, community energy flows are predicted to vary with several climate and anthropogenic variables. Temperature, seasonality, and other factors associated with the tropical-temperate gradient will likely correlate, particularly as strong climate-energy relationships have been observed in small mammals at both the species and community levels (Lovegrove 2003, Naya et al. 2013, Carter and Alroy 2022). In addition, anthropogenic factors including human population density, economic health, and different land use categories may also correlate due to the overall detrimental effects humans have on ecological communities (Maurer 1996, Newbold et al. 2015).

Materials & Methods

Samples and species

Ecological camera trap inventories were downloaded on 10 June 2022 from the Ecological Register database (http://ecoregister.org, see Alroy 2015, 2017, Carter and Alroy 2022). Each sample corresponds to one inventory consisting of a list of species with a matching count of photographs from a particular geographical location. Samples were entered into the register from published camera trap studies, with species names taxonomically standardised across samples by carefully consulting the most recent published taxonomic research. Photo counts are routinely corrected for multiple occurrences of the same individuals in the camera trap literature (Sollmann 2018). Upon entry, each species was assigned to a distinct ecological group such as 'carnivore', 'rodent', or 'other large mammal'. The initial download consisted of 246 samples that contained any species of carnivores, primates, rodents, ungulates, other large mammals, or other small mammals. These six ecological groups correspond to one or more different taxonomic groupings; species belonging to less diverse taxonomic orders are combined into larger non-taxonomic groupings based on their similar ecological roles. The first three categories represent the orders Carnivora, Primates, and Rodentia, respectively. The ungulates include perissodactyls, terrestrial artiodactyls, and proboscideans. The other large and other small mammals include various other groups such as marsupials, lagomorphs, lipotyphlans, hyraxes, pangolins, and xenarthrans. All terrestrial non-volant mammal groups were thus included in the download.

Across the six ecological groups, only species with an average adult body weight of 1 kg or more were included. The was done because large mammal communities were the focus of this study, and horizontally-mounted camera traps do not reliably detect small species (Thomas et al. 2020). This cutoff brought the raw species count of 612 down to 447 (see Appendices S1–S3).

When there were instances of replicate samples – usually representing different seasons or years of a single camera trap survey – only the largest sample (in terms of total abundance) was downloaded. Specifically, samples were deemed replicates if they were from the same published paper and had the same habitat type, altered habitat, and disturbance category plus identical area coordinates (0.1 by 0.1 degrees across). In order to standardise for variation in sampling effort among sites, the number of records per species was divided by the total number of trap nights for each sample. It was possible to calculate these 'count-per-day' units for all but five of the downloaded samples. Excluding them brought the total number of analysed samples to 241.

Species abundances therefore reflect the number of captures per day and per trap for each site. Note that the species pool of each sample is drawn from a single location and habitat type, with each camera trap corresponding to a virtual line transect: the core difference being that here the animals themselves walk into the radius of the traps over a fixed period of time, instead of an observer walking out literal transects with a particular radius over a fixed period of time. As such, the number of trap days effectively standardises by area. Because the sample points (camera traps) are scattered throughout a site of a specific habitat type, small-scale variation in population density is also averaged out. Furthermore, while species detection rates likely vary across samples, complete inventorying of all species present in a community is not required as the data are abundance-weighted. Any rare species that happened not to have been captured would have had a low abundance even if it was detected, and thus would have had little effect on the calculated rate of community energy flow. Therefore, each sample is representative of a single, local community, and samples are fully comparable with each other. Indeed, there are only very weak negative correlations between sampling effort and calculated per-day and per-trap rates of energy flow and mass (see Fig. 1, $R^2 < 5\%$ in all comparisons).

Body mass and metabolic rate

Most species (327) had an average body mass measurement already recorded in the Ecological Register. These were all taken from published measurements of wild, adult individuals. For the remaining species, masses were obtained from the primary literature or from the Encyclopedia of Life online database (https://eol.org, Parr et al. 2014). In addition to the 447 identified species, 36 indeterminate species (denoted with 'sp.' or 'spp.') were also included. Their masses were calculated by taking the geometric mean for congeners present in the Ecological Register (Appendix S2).

Basal metabolic rate (BMR) – the rate of energy consumption of a resting, post-absorptive adult in a thermo-neutral environment (McNab 1997) – was obtained from primary literature. BMR is by far the most common and available rate measure, and is a highly useful signal that correlates with other rate measures including field metabolic rate (White and Seymour 2004). Furthermore, BMR allometrically scales with body mass with exponent values ranging from 2/3 to 3/4 (White and Seymour 2005), similar to other rates (Nagy 2005, Hudson et al. 2013). As a result, while the subsequent rates of community energy flow calculated only represent the community at basal metabolic levels, the significant relationships and variation in rates recovered should not considerably differ to those scaled up from other rate measures.

In total, BMR was directly obtained for 141 out of the 447 species (Appendix S2). The BMRs of the remaining species, including the indeterminate ones, were estimated from body mass based on observed allometric scaling relationships (White 2011). To account for the effects of phylogeny, BMRs for the majority (297) of the 306 species without directly obtained measures were estimated using the PHYLACINE phylogeny (v. 1.2.1, Faurby et al. 2018, 2020) and PhyloPars web server tool (ibi.vu.nl/programs/phylopars/, Bruggeman et al. 2009, see Supporting Information). For the remaining nine species, BMRs were predicted based on an ordinary least squares regression model calculated for the 141 species with direct mass and BMR measurements (Table S1, Fig. S1, Supporting Information). The model was calculated with life form (i.e. ecological group) as a second predictor, with BMRs for the remaining nine species, plus the 36 indeterminate sp. records, predicted using the specific model coefficients of their respective ecological groups (Table S1, Supporting Information). Mass and BMR were both $\log_{10}$-transformed, and all BMRs were predicted in units of ml O_2 h^{-1}. These were converted into kJ day^{-1} using the conversion factor 1 kJ hr^{-1} = 47.8 ml O_2 h^{-1} (Supporting Information in Fristoe et al. 2015).

Sample records and community energy flows

Before rates of community energy flow were calculated, the sample records file was screened to remove all records of domesticated or invasive species. This was done so rates of energy flow would be indicative of 'natural' communities before the introduction of domesticates and non-native species by humans. Furthermore, while such species undoubtedly contribute to community energy flows, there is substantial variation in the number of domesticated and invasive species that are recorded between camera trap surveys, depending on where they are conducted. For example, many Australian samples contain high abundances of domesticates and invasives as there are more surveys from highly anthropogenically-altered landscapes, such as cattle ranches, than in southeast Asia, where the majority of surveys are from natural tropical rainforests. Thus, these species

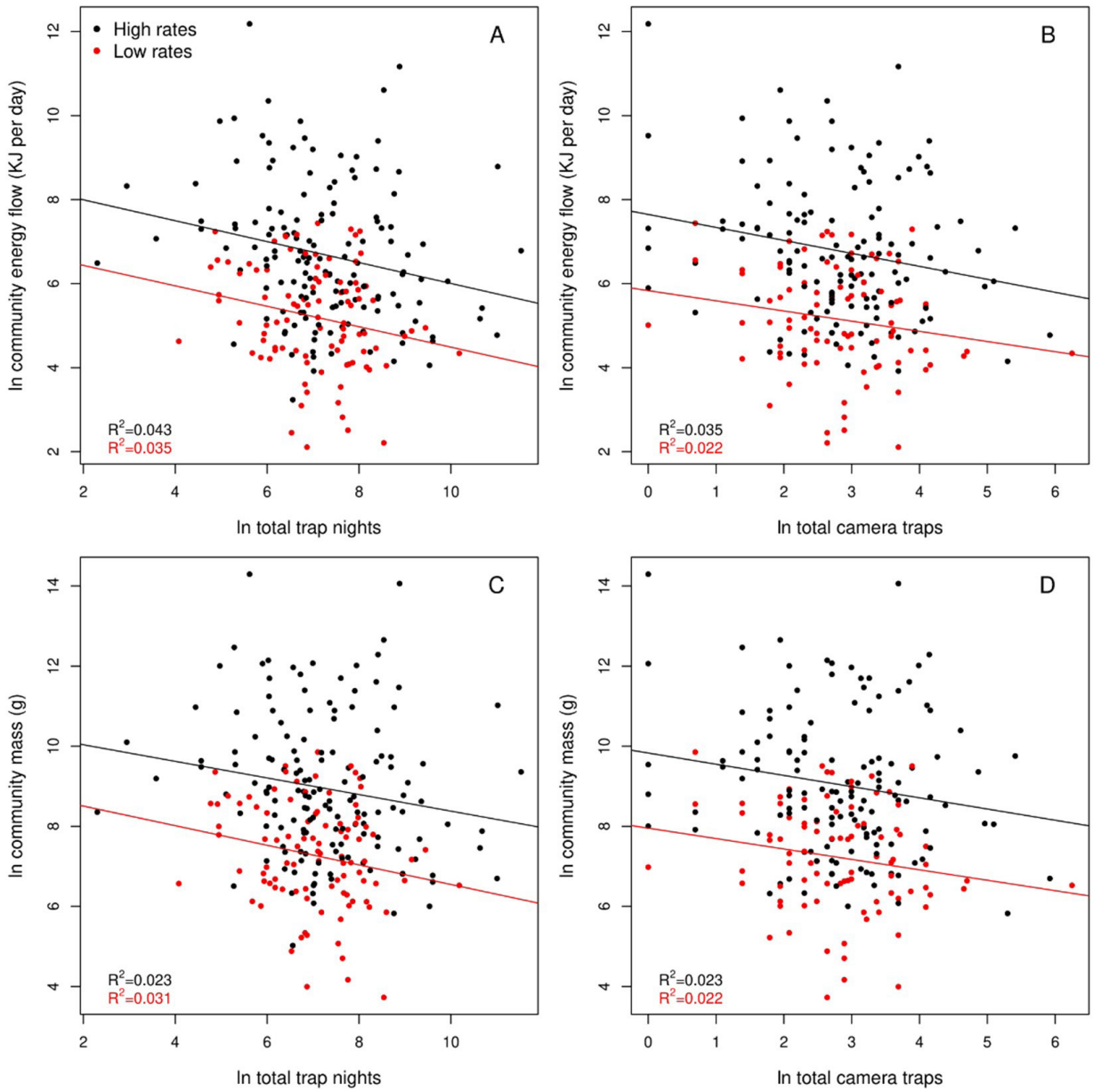

Figure 1. Calculated rates of community energy flow (A and B) and community mass (C and D) compared with the total numbers of camera trap nights (A and C) and total numbers of camera traps (B and D) for all 241 samples. All variables are logged. The point and line colours separate the regions with high rates of energy flow and mass (black) from those with low rates and masses (red). The former regions are the Nearctic, Afrotropics, Indomalaya, and the eastern Palearctic (n = 146) and the latter are the Neotropics, Australasia, and western Palearctic (n = 95).

were removed to also control for such variation. Five domesticates (*Bos taurus*, *Bubalus bubalis*, *Equus africanus asinus*, *Felis catus*, *Ovis aries*) and one invasive species (*Ammotragus lervia*, found only in North America in this dataset) were removed entirely, and a further 13 species were partially removed based on geography. All indeterminate records were also removed. Thus, the final analysis consisted of 441 species, 241 samples, and 2981 species-plus-sample combinations (Appendices S1–S3).

As camera trap data are often biased by variation in detection probability among species (Rowcliffe et al. 2008, Wong et al. 2019), which are notably higher for carnivorous and larger bodied species as they move greater distances (Cusack et al. 2015), the abundances were further corrected by dividing per-day trap rates by estimated daily path lengths (i.e. the average distance travelled by an animal in a day). As there were only 75 large mammal species with path lengths (PLs) available in the primary literature, most species had their PL estimated from body mass. The same procedure used to predict BMRs described above, was used to predict PLs, with the majority (370) being estimated using the PhyloPars website. The remaining 12 species had their PL calculated using OLS regression coefficients, again with life

form as a second predictor, if they did not already have a direct PL measurement (see Supporting Information).

The rate of community energy flow (EF_{com}) was calculated for each sample using the equation:

$$EF_{com} = \sum_{i=1}^{n} \left(N_i * M_i \right) \left[\text{kJ trap}^{-1} \text{ day}^{-2} \right]$$

where n is the number of species in the sample, N_i is the abundance of species i, measured by count per trap per day and corrected by path length, and M_i is the metabolic rate of a species, measured in kilojoules per day (kJ day^{-1}). In other words, the rate of energy flow of a community is the product of the abundance and metabolic rate of each constituent species summed across all species in the sample.

In addition, the per-gram rate of community energy flow (kJ g^{-1} trap^{-1} day^{-1}) was calculated for each sample by taking the ratio between total community energy flow and total community mass. Community mass was calculated using the same total energy flow equation above, only with mass being substituted for metabolic rate, and was measured in grams per trap per day (g trap^{-1} day^{-1}). As the per-gram rate of community energy flow is analogous to the individual mass-specific metabolic rate, which is greater in smaller organisms due to the allometric scaling of BMR, two more metrics were calculated to distinguish between the effects of body size and abundance: an abundance-weighted average individual rate of energy flow (kJ trap^{-1} day^{-1}) and an abundance-weighted average individual mass (g). These represent the typical rate of energy flow and mass, respectively, of an average individual in that community. Both were calculated by dividing the total community energy flow or total community mass by the total abundance (total count per trap per day) of the community. All five calculated metrics were analysed separately (see Fig. 1 in Carter and Alroy (2022) for an illustration of how each metric was calculated).

Predictor variables

There were four climate variables, two environmental variables, seven anthropogenic variables, six binary geographic variables, and one species richness estimate variable, for a total of 20 independent predictors. The climate data were obtained from the WorldClim database (https://www.worldclim.org, Fick and Hijmans 2017) if such data could not be drawn directly from the primary literature. This included mean annual temperature (MAT), mean annual precipitation (MAP), temperature annual range (TAR), and precipitation seasonality (PS). MAT and MAP are recorded in the Ecological Register, and pertain to the individual sample locations whenever possible. If not, climate values for the closest possible locations are often recorded. The MAP data were square-root transformed because this normalised the data better than log-transforming. The two environmental variables, actual evapotranspiration (AET) and net primary productivity (NPP), were obtained from TerraClimate (Abatzoglou et al. 2018) and SEDAC (Imhoff et al. 2004, Imhoff and Bounoua 2006), respectively. The anthropogenic variables comprised human population density (HPD), per capita GDP based on purchasing power parity (PPP), and four land use categories: urban, village, croplands, and rangelands. These were also obtained from SEDAC (Nordhaus 2006, Nordhaus and Chen 2016, Ellis and Ramankutty 2008a, 2008b). PPP was log-transformed, and the population density data were Yeo-Johnson transformed (Yeo and Johnson 2000) because they included zero values and so they could not be logged. The value for the four land use variables for each sample was the proportion of 25 evenly spaced points within each surrounding 1 x 1° cell that fell within the relevant category. A binary 'protected' variable, representing whether a given site is legally protected from disturbance (e.g. within a national park), was also included. Lastly, the six binary geographic variables represented each of the six main biogeographical realms: the Afrotropics, Australasia, Indomalaya, Nearctic, Neotropics, and Palearctic.

Species richness was estimated using the geometric series (GS) index (Kerr and Alroy 2023, Appendix S4). Like other indices, the GS index estimates the number of missing species by extrapolating on the basis of counts of individuals per species. For example, Chao 1 (Chao 1984) focuses on species that have counts of one or two (i.e. singletons or doubletons). Unlike other methods, the GS index considers all species counts at once to estimate richness, and it extrapolates more strongly when the counts are closer to zero. The index also assumes that counts are unevenly distributed, whereas Chao 1 assumes counts are uniformly distributed (Alroy 2017). A full breakdown of the GS index along with analytical tests comparing it to other richness metrics are provided in Kerr and Alroy (2023). Richness was calculated for 230 of the 241 samples. The remainder all had less than four count classes and so richness could not be reliably estimated.

Statistical analyses

All analyses were conducted using R v.4.2.2 (R Core Team 2022). Each of the five dependent variables were logged and compared to the 20 predictors using three separate analytical methods: model selection, least-squares orthogonalization regression (see below), and spatial autoregression. Model selection was performed using the package *BeSS* (Wen et al. 2020). All possible counts of predictors were enumerated, with each model selecting the subset of all linear model scores with the lowest Bayesian information criterion (BIC) value.

Least-squares orthogonalization (LSO) regression (see Gibson 1962, Johnson 1966, Green et al. 1978) was conducted to account for the high level of collinearity between several of the predictors (e.g. MAT and TAR), an issue that can often bias analyses with many confounding factors (Dormann et al. 2013). LSO regression rotates the predictor variables to render them mutually orthogonal, meaning that each pair ends up being entirely uncorrelated. The method is distinctive because the predictors are rotated minimally, preserving their values as much as possible.

The rotated predictors can be interpreted as latent variables analogous to those produced by factor analysis, but they are much more easily interpretable. The total variance explained by LSO regression is exactly the same as that explained by the original variables, with the slopes being more interpretable. The method is completely distinct to other methods that involve orthogonalization such as the Gram–Schmidt process, or to Graham's (2003) sequential regression method that was used in Carter and Alroy (2022). Lastly, in order to control for the potential influence of spatial autocorrelation (Lichstein et al. 2002), the orthogonalized variables were also analysed using spatial autoregression with the package *spatialreg* (Bivand and Piras 2015). Thus, there were a total of 15 separate analyses. Due to the large number of predictors, the significance level was set at $\alpha = 0.001$ and *p*-values between 0.001 and 0.01 were considered marginal.

Results

Total energy flow and mass

The results for total community energy flow and community mass were highly similar across all analyses due to their strong and positive mutual relationship. The total energy use of a community is primarily determined by its overall mass, with energy flow of large mammal communities scaling to mass with an exponent of 0.922 ($R^2 = 0.9752$, $p < 0.0001$, Fig. 2), as defined by computing a standard major axis regression constructed with package *smatr* (Warton et al. 2012). The Neotropics variable was the most consistent in explaining each one, presenting a strongly negative slope in all analyses (Tables 1-2, S2-S3, Fig. 3). These were contrasted by strong positive relationships with the Afrotropics variable in the LSO and spatial regressions for both metrics, in addition to positive relationships with TAR (Tables 2, S2-S3). Richness was also selected in the BeSS model for community mass alongside the Afrotropics variable (Table 1).

Per-gram rate of energy flow

For per-gram rate of energy flow (total energy flow divided by total mass), the most striking result across all analyses was a strong negative relationship with species richness (Tables 1-2, S4). Less speciose communities have higher rates of energy flow relative to mass than those with a greater number of species. Alongside richness, there were positive relationships with the Neotropics variable in all analyses (strong in the case of LSO) and with human population density, although the latter was only marginal in the LSO and

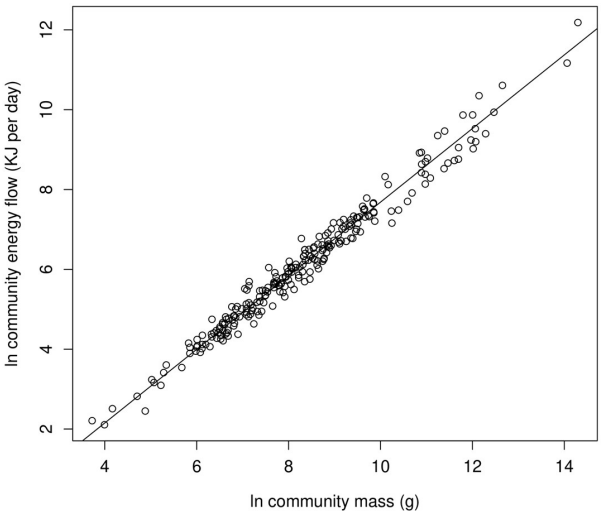

Figure 2. A standard major axis regression of log community energy flow and log community mass for all 241 ecological samples ($p < 0.0001$, slope = 0.922, $R^2 = 0.9752$).

Table 1. The slopes, *t*-values, *p*-values, and R^2s for the variables selected in BeSS analyses of total energy flow, total mass, per-gram energy flow, individual energy flow, and individual mass.

Model (BIC)	Variable	Slope	*t*	*p*	R^2
Total energy flow (176.97)	Neotropics	-1.6376	-7.310	< 0.0001	0.1925
Total mass (213.55)	Afrotropics	0.3918	1.162	0.2464	0.2293
	Neotropics	-1.7951	-7.127	< 0.0001	
	Richness	0.4948	2.414	0.0166	
Per-gram energy flow (-585.69)	Neotropics	0.2263	5.696	< 0.0001	0.3208
	HPD	0.0308	3.385	0.0008	
	Richness	-0.2644	-8.502	< 0.0001	
Individual energy flow (-57.38)	Neotropics	-1.0258	-7.427	< 0.0001	0.3104
	TAR	0.0181	2.786	0.0058	
	Urban	-1.7249	-1.955	0.0518	
	Richness	0.4893	4.225	< 0.0001	
Individual mass (37.00)	Neotropics	-1.3788	-8.555	< 0.0001	0.3036
	Urban	-2.8825	-2.634	0.0090	
	Richness	0.5995	4.545	< 0.0001	

Table 2. The statistically significant independent variables yielded by each of the least-squares orthogonalization regressions. Non-significant variables are excluded. The beta coefficients are the slopes standardised by the standard deviations of the variables.

Dependent variable (units)	Predictor	Beta coefficient	*t*	*p*	R^2
Total energy flow (kJ day^{-2})	Afrotropics	0.2077	3.427	0.0007	0.2650
	Neotropics	-0.3572	-5.892	< 0.0001	
	TAR	0.1824	3.010	0.0029	
Total mass (g day^{-1})	Afrotropics	0.2271	3.813	0.0002	0.2905
	Neotropics	-0.3695	-6.203	< 0.0001	
	TAR	0.1707	2.865	0.0046	
Per-gram energy flow (kJ g^{-1} day^{-1})	Afrotropics	-0.2091	-3.7206	0.0002	0.3680
	Neotropics	0.2394	4.259	< 0.0001	
	HPD	0.1457	2.592	0.0102	
	Urban	0.1968	3.502	0.0005	
	Richness	-0.4008	-7.131	< 0.0001	
Individual energy flow (kJ day^{-1})	Indomalaya	0.1845	3.302	0.0011	0.3756
	Neotropics	-0.3839	-6.870	< 0.0001	
	TAR	0.1839	3.291	0.0011	
	Urban	-0.1520	-2.720	0.0071	
	Richness	0.1993	3.567	0.0004	
Individual mass (g)	Afrotropics	0.1446	2.586	0.0104	0.3751
	Indomalaya	0.1677	3.000	0.0030	
	Neotropics	-0.3678	-6.579	< 0.0001	
	TAR	0.1524	2.727	0.0069	
	Urban	-0.1709	-3.057	0.0025	
	Richness	0.2594	4.641	< 0.0001	

spatial regressions (Tables 1-2, S4, Fig. 3B). These were accompanied by positive and negative relationships with the Urban and Afrotropics variables, respectively, in the LSO and spatial regressions (Tables 2, S4).

Abundance-weighted individual energy flow and mass

There were four consistent relationships involving abundance-weighted individual rate of energy flow (total energy flow divided by total community abundance): positive relationships with species richness and TAR, and negative relationships with the Neotropics variable and the proportion of urban area (Tables 1-2, S5). The Neotropics signal was very strong in the LSO analysis (Table 2). There were also positive relationships with the Indomalaya variable in the LSO and spatial regressions (Tables 2, S5).

For abundance-weighted individual mass (total mass divided by total abundance), the observed relationships with individual energy flow were mostly repeated in all analyses (Tables 1-2, S6). There were only a few differences: TAR was not selected in the BeSS model (Table 1) and there was a marginally positive slope for the Afrotropics variable in the LSO regression (Table 2). Otherwise, the results were largely identical to those seen with individual energy flow. The strongest results, based on the LSO analyses, are the much lower average individual rates and masses in the Neotropics (Table 2).

Discussion

This discussion is structured to address the main hypotheses about each of the broad variable categories outlined in the introduction. These relate to biogeography, species richness, climate, and anthropogenic factors. Overall, the main finding is that community energy flow and mass are relatively low in the Neotropics and high in the Afrotropics.

Biogeographic patterns

Total energy flow and mass

Geographic variation in total community energy use is a primary signal in the data (Fig. 3). Biogeographic variables are the only consistent predictors across all sets of analyses (Tables 1-2). Furthermore, the results match the predictions, with rates being significantly higher in a realm where megafauna are still common (the Afrotropics) and significantly lower where megafauna are absent or much less abundant (the Neotropics: Tables 1-2, Fig. 3A). These patterns are mirrored by total community mass because it closely tracks community energy flow (Fig. 2). Notably, similar Afrotropical–Neotropical splits have been recovered in previous studies, for instance in an analysis of phylogenetic

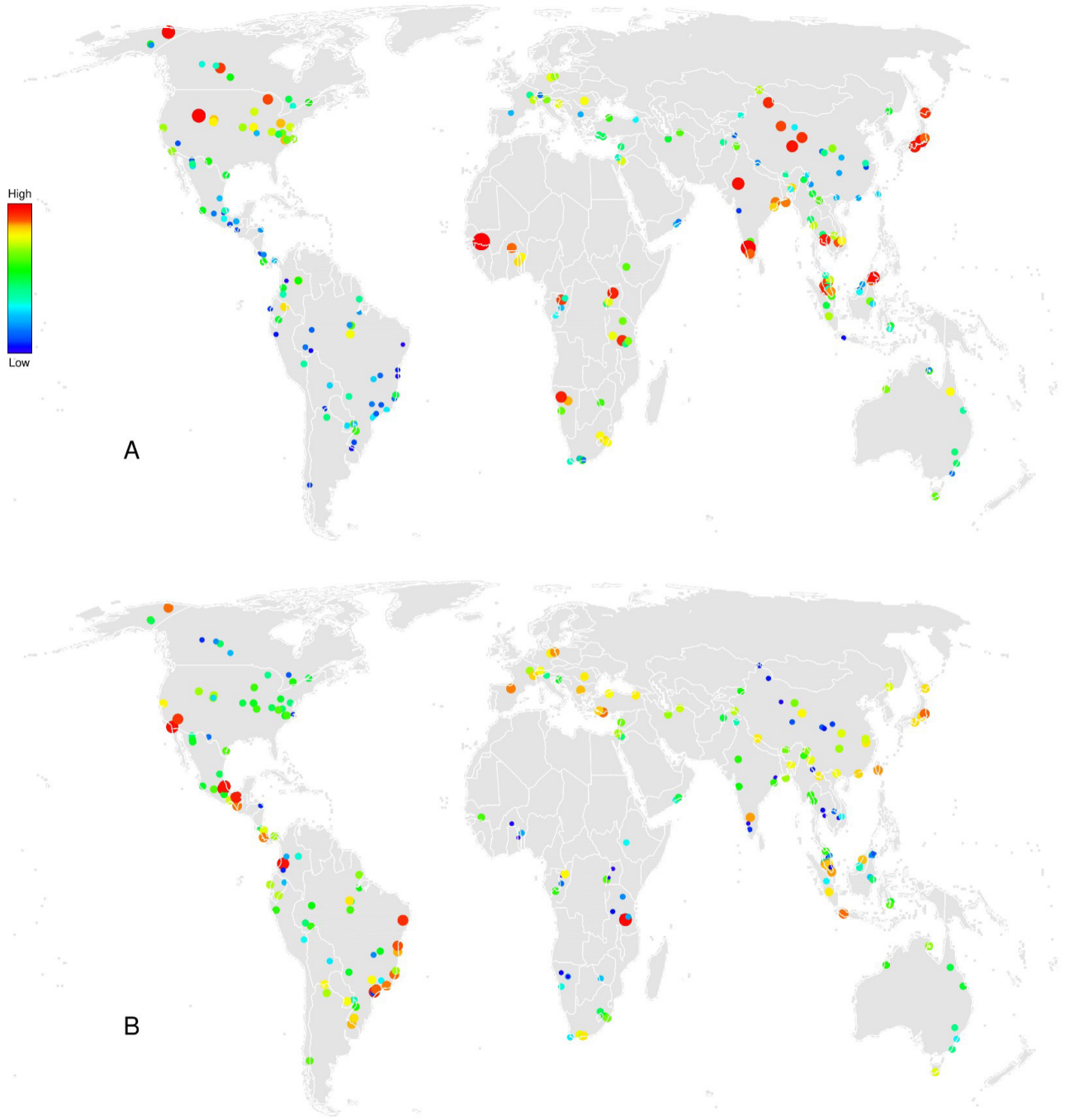

Figure 3. The relative strength of (A) total energy flows and (B) per-gram energy flows for 241 large mammal communities. The colour and size of the circles represent the strength of energy use, with small blue circles indicating low values and large red circles indicating high ones. The circle colour and sizes are based on logged and scaled data.

and functional trait diversity in tropical large mammal communities (Rowan et al. 2020). Crucially, these patterns bear no relationship to variation in sampling effort among realms (Fig. 1).

As noted above, megafauna (species ≥ 45 kg) were common in all major biogeographic realms before the Late Pleistocene extinctions (Martin 1967, 1984, Smith et al. 2018, 2019). These extinctions were unique both in their extreme selectivity with respect to body size (Alroy 1999, Smith et al. 2018) and in their variable severity across continents (Barnosky et al. 2004, Koch and Barnosky 2006). South America was the most impacted, with a loss of around 50 megafaunal genera, 62 large mammal species, and three entire orders weighing over 10 kg (Koch and Barnosky 2006, Sandom et al. 2014). In Australia, 23 terrestrial megafaunal genera died out in total (Roberts et al. 2001), including 26 large

mammal species (Sandom et al. 2014) and entire ecological guilds. In contrast, Africa and Eurasia each only lost around 10 megafaunal genera, or about 20 large mammal species (Koch and Barnosky 2006). The greater extinction severity in the Americas and Australia has long been attributed to the naiveté of prey to human hunters following their arrival on these continents (Martin 1967, 1984). This contrasts with the much longer period of hominin-megafauna coevolution in Africa and Eurasia (Stiner 2002). These patterns are therefore consistent with a human cause of the extinctions (Martin 1967, 1984, Sandom et al. 2014, Saltré et al. 2016, Araujo et al. 2017).

In general, the biogeographic patterns of community energy use match the spatial distribution of megafaunal extinction intensity (Fig. 3A). In addition to the striking contrast between the Neotropics and Afrotropics, total rates are also consistently lower in Australasia (Fig. 3A), although the effect was not statistically significant likely because there were few Australasian samples, and several had to be omitted from the analyses. The omitted samples only contained two or three native species over 1 kg in weight, making it impossible to compute meaningful species richness estimates. The lack of surviving megafauna and low abundances of native species explains why Australasian rates are visibly low, although are not significant (Tables 1-2). Furthermore, within Eurasia, energy use is lower in Europe (Fig. 3A), which becomes a notable extinction hotspot when later Holocene extinctions of large mammals are included (Sandom et al. 2014). Indeed, the regions that have experienced the greatest proportion of large mammal extinctions over the past 130,000 years generally have the most consistently reduced rates of community energy flow (Fig. 3A, see also Fig. 1 in Sandom et al. 2014). This strongly suggests that large mammal extinctions are the ultimate and fundamental determinant of modern community energy use patterns.

However, there is an interesting anomaly. Despite numerous terminal Pleistocene species extinctions, the Nearctic realm does not present reduced rates of community energy use or lower total masses (Tables 1-2). In North America, 38 mostly megafaunal genera and 43 species went extinct, obliterating two entire orders (Koch and Barnosky 2006, Sandom et al. 2014, Meltzer 2020). The discrepancy is probably due to the high contemporary abundances of certain large species such mule deer, white-tailed deer, and caribou (Appendix S3). These highly abundant species have no equivalents in the Neotropics and Australasia, and their presence clearly results in Nearctic communities having greater variation in rates of energy use when compared to the former two realms (Fig. 3A). Indeed, considerable variation in rates should be present within each realm that reflects continental variation in mammalian communities, as is clearly seen in Africa and Eurasia (Fig. 3A). The surprising uniformity of rates in Australasia and the Neotropics therefore highlights the severely homogenizing effects the absence of abundant large mammals has had in these regions. Notably, deer populations in North America were severely reduced by overhunting in the 19th and early 20th centuries (McCabe and McCabe 1984). Thus, the energy use and mass of Nearctic communities would likely be similar to the other highly-impacted regions if not for the successful introduction and implementation of hunting regulations and conservation programs.

Per-gram rates and individual metrics

Per-gram rates of community energy flow also indicate differences between regions that mirror Pleistocene extinctions. Specifically, per-gram rates are low in the Afrotropics and high in the Neotropics (Tables 1-2, Fig. 3B). The relationships are reversed relative to those involving total energy flow, just as they are on the organismal level (Hulbert and Else 2000, Savage et al. 2007). Per-gram rates are high in the Neotropics because communities include many smaller individuals with high mass-specific metabolisms, in contrast to Afrotropical communities, which comprise greater abundances of larger species (Table 2, Appendix S3).

Per-gram rates are also different in the most impacted regions. Australasian communities have reduced total rates, as in the Neotropics, but do not have correspondingly high per-gram rates (Fig. 3B). This is likely due to differences in average abundances. Australasian communities do not feature large numbers of small individuals that are > 1 kg, as indicated by the absence of relationships with individual mass (Tables 1-2). They instead simply include fewer native individuals in general (Appendix S3). Furthermore, marsupials are known to have consistently low BMRs (McNab 1986, 2005). As a consequence, Australasian communities should have lower rates of energy flow relative to their mass, and this likely results in the absence of high per-gram rate communities despite exhibiting low total rates (Fig. 3). Lastly, the positive slopes for the Afrotropics and Indomalaya variables seen in the individual metrics further indicates that the high community rates seen in these realms are due to the relatively higher abundances of true megafauna (Table 2).

Species richness patterns

Although there are no relationships between species richness and total energy flow, richness bears strong negative relationships with per-gram rates and positive relationships with the two individual metrics (Tables 1-2, S4-S6). Thus, reduced diversity is directly associated with the absence of large species. In other words, only the more species-rich communities contain megafauna, and thus exhibit low per-gram rates. As larger species are more prone to extinction (Brook and Bowman 2005, Ripple et al. 2019) – and have continued to go extinct since the Late Pleistocene (Braje and Erlandson 2013, Smith et al. 2018) – their loss not only results in reduced diversity, but their outsized effects lead to strong increases in per-gram rates when they are removed, as subsequently less species-rich communities are comprised mainly of smaller organisms (Tables 1-2).

Climate and anthropogenic patterns

The only significant climate predictor was TAR, a marginal and positive term in the LSO and spatial

regressions for the community-wide and individual-based metrics (Tables 2, S2-S6). The lack of any truly strong relationships means that climate is uncoupled from energy flow in large mammal communities, unlike small mammal communities (Carter and Alroy 2022). While high rates occur in the Nearctic and eastern Palearctic, likely resulting in the positive relationships with TAR, they are consistently low in Europe (Fig. 3A). Such clear differences among communities found at similar latitudes, even within a single geographic realm, further supports the idea that variation in energy use reflects variation in large-mammal extinction intensity.

The main anthropogenic predictors were the proportion of urban area and, to a lesser extent, human population density, both relating positively to per-gram rates (Tables 1-2). Urban area also relates negatively to both of the individual-based metrics (Tables 1-2). Thus, reduced individual rates of energy flow and mass directly yield higher per-gram rates in native urban communities. This could partly be a result of urban domesticates or invasive species suppressing the occurrences of natives to an extent that only a handful of small native species are detected, thus increasing per-gram rates. Surprisingly, there were no significant relationships recovered with the protected area variable on either the community or individual levels (Tables 1-2, S2-S6). The lack of any effect of protected areas is likely due to the persistence of various anthropogenic stressors (Mora and Sale 2011, Ferraro et al. 2013), and conversely the frequent persistence of high species abundances in unprotected areas. Despite the absence of a relationship with total energy use, the urban area results still highlight the detrimental effects of anthropogenic disturbances.

Conclusion

Biogeographic patterns are the primary control on large mammal community energy use around the world. These most likely relate to the megafaunal extinctions of the Late Pleistocene, reflecting spatial variation in their impacts. This study therefore adds to a growing body of recent literature highlighting how the varying intensity of Late Pleistocene extinctions has altered modern macroecological patterns in various ways, with others including latitudinal body mass distributions and tropical community composition (Faurby and Araujo 2017, Rowan et al. 2020). While the most devastated regions continue to have the most reduced rates of energy flow and biomass, there are further differences in energy use patterns between realms. These are driven by fundamental differences in abundances, metabolism, and ecology. Geographical differences greatly outweigh the impacts of other factors, and they clearly result from the highly selective extinction of large-bodied mammals (Brook and Bowman 2005, Sandom et al. 2014, Smith et al. 2018). The fragility and ecological importance of surviving megafaunal species underscores the importance of conserving them. If the largest ones are lost, then rates of energy use will be substantially reduced across the globe, which will have severe and wide-ranging ecological consequences (Estes et al. 2011, Smith et al. 2019, Forbes et al. 2019, Enquist et al. 2020). The fact that Pleistocene extinctions are mirrored by current-day energy use patterns suggests that further reductions will likely persist for thousands of years. Thus, successful preservation of extant megafauna is essential for limiting future impacts.

Acknowledgments

We thank Barry Brook and Kate Lyons for helpful advice, and Orlin S. Todorov for valuable assistance in estimating basal metabolic rates using phylogenetic methods. This study was funded through a Research Training Program Scholarship (no. 20213308 awarded to BEC) and a Discovery Project Award from the Australian Government (no. DP210101324 to JA).

Author Contributions

BEC designed the study, downloaded the sample data, collated and calculated the metabolic rate data, calculated rates of community energy flow, and performed the analyses with assistance from JA. JA obtained the majority of the sample data with assistance from BEC, obtained the path length, climate, and anthropogenic variable data, and developed the species richness estimation method. BEC wrote the manuscript and JA edited the manuscript.

Data Availability Statement

The data and R code supporting the results are available online as part of the Supplemental Material for this article.

Supplemental Material

This material is available as part of the online article from https://escholarship.org/uc/fb

Figure S1. The relationship between log10 mass (g) and log10 basal metabolic rate (BMR; ml O_2 h^{-1}) as defined by OLS regression.

Table S1. The coefficients of the body mass-BMR regression model for the 141 species with actual BMR measures when adding life form (ecological group) as a second predictor. [[Q1: Q1]]

Table S2. The slopes, z, and p-values for the multiple spatial autoregression based on total community energy flow.

Table S3. The slopes, z, and p-values for the multiple spatial autoregression based on total community mass.

Table S4. The slopes, z, and p-values for the multiple spatial autoregression based on per-gram community energy flow.

Table S5. The slopes, z, and p-values for the multiple spatial autoregression based on the average abundance-weighted rate of individual energy flow.

Table S6. The slopes, z, and p-values for the multiple spatial autoregression based on average abundance-weighted individual mass.

Appendix S1. The complete list of all 241 large mammal camera trap samples downloaded from the Ecological Register and used in the analysis.
Appendix S2. The body mass, path length, and basal metabolic rate of all 447 species > 1 kg that were present in the initial sample download. The values for the 36 indeterminate species records are also listed.
Appendix S3. The complete ecological register containing all 2981 species-plus-sample combinations, including body mass, path length, and basal metabolic rate for each species.
Appendix S4. R code for conducting the analyses. Includes the geometric series richness estimator and the least-squares orthogonalization (LSO) regression method.

References

Abatzoglou, J.T., Dobrowski, S.Z., Parks, S.A. & Hegewisch, K.C. (2018) TerraClimate, a high-resolution global dataset of monthly climate and climatic water balance from 1958-2015. Scientific Data, 5, 170191. https://doi.org/10.1038/sdata.2017.191

Alroy, J. (1999) Putting North America's end-Pleistocene megafaunal extinction in context. In: Extinctions in near time: causes, contexts, and consequences (ed. by R.D.E. MacPhee), pp. 105-143. Springer, Boston, MA.

Alroy, J. (2015) The shape of terrestrial abundance distributions. Science Advances, 1, e1500082. https://doi.org/10.1126/sciadv.1500082

Alroy, J. (2017) Effects of habitat disturbance on tropical forest biodiversity. Proceedings of the National Academy of Sciences USA, 114, 6056-6061. https://doi.org/10.1073/pnas.1611855114

Araujo, B.B.A., Oliveira-Santos, L.G.R., Lima-Ribeiro, M.S., Diniz-Filho, J.A.F. & Fernandez, F.A.S. (2017) Bigger kill than chill: the uneven roles of humans and climate on late Quaternary megafaunal extinctions. Quaternary International, 431, 216-222. https://doi.org/10.1016/j.quaint.2015.10.045

Barneche, D.R., Kulbicki, M., Floeter, S.R., Friedlander, A.M., Maina, J. & Allen, A.P. (2014) Scaling metabolism from individuals to reef-fish communities at broad spatial scales. Ecology Letters, 17, 1067-1076. https://doi.org/10.1111/ele.12309

Barnosky, A.D., Koch, P.L., Feranec, R.S., Wing, S.L. & Shabel, A.B. (2004) Assessing the causes of Late Pleistocene extinctions on the continents. Science, 306, 70-75. https://doi.org/10.1126/science.1101476

Barnosky, A.D., Matzke, N., Tomiya, S., et al. (2011) Has the Earth's sixth mass extinction already arrived? Nature, 471, 51-57. https://doi.org/10.1038/nature09678

Bivand, R. & Piras, G. (2015) Comparing implementations of estimation methods for spatial econometrics. Journal of Statistical Software, 63, 1-36. https://doi.org/10.18637/jss.v063.i18

Braje, T.J. & Erlandson, J.M. (2013) Human acceleration of animal and plant extinctions: a Late Pleistocene, Holocene, and Anthropocene continuum. Anthropocene, 4, 14-23. https://doi.org/10.1016/j.ancene.2013.08.003

Brook, B.W. & Bowman, D.M.J.S. (2005) One equation fits overkill: why allometry underpins both prehistoric and modern body size-biased extinctions. Population Ecology, 47, 137-141. https://doi.org/10.1007/s10144-005-0213-4

Brown, J.H., Gillooly, J.F., Allen, A.P., Savage, V.M. & West, G.B. (2004) Toward a metabolic theory of ecology. Ecology, 85, 1771-1789. https://doi.org/10.1890/03-9000

Bruggeman, J., Heringa, J. & Brandt, B.W. (2009) PhyloPars: estimation of missing parameter values using phylogeny. Nucleic Acids Research, 37, W179-W184. https://doi.org/10.1093/nar/gkp370

Cardillo, M., Mace, G.M., Jones, K.E., Bielby, J., Bininda-Emonds, O.R.P., Sechrest, W., Orme, C.D.L. & Purvis, A. (2005) Evolution: multiple causes of high extinction risk in large mammal species. Science, 309, 1239-1241. https://doi.org/10.1126/science.1116030

Carter, B.E. & Alroy, J. (2022) The macroecology of community energy use in terrestrial vertebrates. Frontiers of Biogeography, 14, e56553. https://doi.org/10.21425/F5FBG56553

Ceballos, G., Ehrlich, P.R., Barnosky, A.D., García, A., Pringle, R.M. & Palmer, T.M. (2015) Accelerated modern human-induced species losses: entering the sixth mass extinction. Science Advances, 1, e1400253. https://doi.org/10.1126/sciadv.1400253

Chao, A. (1984) Nonparametric estimation of the number of classes in a population. Scandinavian Journal of Statistics, 11, 265-270. https://www.jstor.org/stable/4615964

Cusack, J.J., Dickman, A.J., Rowcliffe, J.M., Carbone, C., Macdonald, D.W. & Coulson, T. (2015) Random

versus game trail-based camera trap placement strategy for monitoring terrestrial mammal communities. PloS ONE, 10, e0126373. https://doi.org/10.1371/journal.pone.0126373

Dirzo, R., Young, H.S., Galetti, M., Ceballos, G., Isaac, N.J.B. & Collen, B. (2014) Defaunation in the Anthropocene. Science, 345, 401-406. https://doi.org/10.1126/science.1251817

Dormann, C.F., Elith, J., Bacher, S., et al. (2013) Collinearity: a review of methods to deal with it and a simulation study evaluating their performance. Ecography, 36, 27-46. https://doi.org/10.1111/j.1600-0587.2012.07348.x

Ellis, E.C. & Ramankutty, N. (2008a) Putting people in the map: anthropogenic biomes of the world. Frontiers in Ecology and the Environment, 6, 439-447. https://doi.org/10.1890/070062

Ellis, E.C., & Ramankutty, N. (2008b) Data from: Anthropogenic biomes of the world, version 1. NASA Socioeconomic Data and Applications Center (SEDAC), Palisades, NY.

Enquist, B.J., Abraham, A.J., Harfoot, M.B.J., Malhi, Y. & Doughty, C.E. (2020) The megabiota are disproportionately important for biosphere functioning. Nature Communications, 11, 699. https://doi.org/10.1038/s41467-020-14369-y

Enquist, B.J., Economo, E.P., Huxman, T.E., Allen, A.P., Ignace, D.D. & Gillooly, J.F. (2003) Scaling metabolism from organisms to ecosystems. Nature, 423, 639-642. https://doi.org/10.1038/nature01671

Ernest, S.K.M. (2005) Body size, energy use, and community structure of small mammals. Ecology, 86, 1407-1413. https://doi.org/10.1890/03-3179

Ernest, S.K.M. & Brown, J.H. (2001) Homeostasis and compensation: the role of species and resources in ecosystem stability. Ecology, 82, 2118-2132. https://doi.org/10.2307/2680220

Estes, J.A., Terborgh, J., Brashares, J.S., et al. (2011) Trophic downgrading of planet Earth. Science, 333, 301-306. https://doi.org/10.1126/science.1205106

Faurby, S. & Araújo, M.B. (2017) Anthropogenic impacts weaken Bergmann's rule. Ecography, 40, 683-684. https://doi.org/10.1111/ecog.02287

Faurby, S., Davis, M., Pedersen, R.Ø., Schowanek, S.D., Antonelli, A. & Svenning, J.C. (2018) PHYLACINE 1.2: the phylogenetic atlas of mammal macroecology. Ecology, 99, 2626. https://doi.org/10.1002/ecy.2443

Faurby, S., Pedersen, R. Ø., Davis, M., Schowanek, S. D., Jarvie, S., Antonelli, A. & Svenning, J.C. (2020) PHYLACINE 1.2.1: an update to the phylogenetic atlas of mammal macroecology. https://doi.org/10.5281/zenodo.3690867

Ferraro, P.J., Hanauer, M.M., Miteva, D.A., Canavire-Bacarreza, G.J., Pattanayak, S.K. & Sims, K.R. (2013) More strictly protected areas are not necessarily more protective: evidence from Bolivia, Costa Rica, Indonesia, and Thailand. Environmental Research Letters, 8, 025011. https://doi.org/10.1088/1748-9326/8/2/025011

Fick, S.E. & Hijmans, R.J. (2017) WorldClim 2: new 1-km spatial resolution climate surfaces for global land areas. International Journal of Climatology, 37, 4302-4315. https://doi.org/10.1002/joc.5086

Forbes, E.S., Cushman, J.H., Burkepile, D.E., Young, T.P., Klope, M. & Young, H.S. (2019) Synthesizing the effects of large, wild herbivore exclusion on ecosystem function. Functional Ecology, 33, 1597-1610. https://doi.org/10.1111/1365-2435.13376

Fristoe, T.S., Burger, J.R., Balk, M.A., Khaliq, I., Hof, C. & Brown, J.H. (2015) Metabolic heat production and thermal conductance are mass-independent adaptations to thermal environment in birds and mammals. Proceedings of the National Academy of Sciences USA, 112, 15934-15939. https://doi.org/10.1073/pnas.1521662112

Gibson, W.A. (1962) Orthogonal predictors: a possible resolution of the Hoffman-Ward controversy. Psychological Reports, 11, 32-34. https://doi.org/10.2466/pr0.1962.11.1.32

Graham, M.H. (2003) Confronting multicollinearity in ecological multiple regression. Ecology, 84, 2809-2815. https://doi.org/10.1890/02-3114

Green, P.E., Carroll, J.D. & DeSarbo, W.S. (1978) A new measure of predictor variable importance in multiple regression. Journal of Marketing Research, 15, 356-360. https://doi.org/10.1177/002224377801500305

Hudson, L.N., Isaac, N.J.B. & Reuman, D.C. (2013) The relationship between body mass and field metabolic rate among individual birds

and mammals. Journal of Animal Ecology, 82, 1009-1020. https://doi.org/10.1111/1365-2656.12086

Hulbert, A.J. & Else, P.L. (2000) Mechanisms underlying the cost of living in animals. Annual Review of Physiology, 62, 207-235. https://doi.org/10.1146/annurev.physiol.62.1.207

Imhoff, M.L. & Bounoua, L. (2006) Exploring global patterns of net primary production carbon supply and demand using satellite observations and statistical data. Journal of Geophysical Research Atmospheres, 111, D22S12. https://doi.org/10.1029/2006JD007377

Imhoff, M.L., Bounoua, L., Ricketts, T., Loucks, C., Harriss, R. & Lawrence, W.T. (2004) Data from: HANPP Collection: Global patterns in net primary productivity (NPP). Palisades, NY: NASA Socioeconomic Data and Applications Center (SEDAC).

Johnson, R.M. (1966) The minimal transformation to orthonormality. Psychometrika, 31, 61-66. https://doi.org/10.1007/BF02289457

Kerr, M.R. & Alroy, J. (2023) Body size and abundance are decoupled from species richness in Australian marine bivalves. Frontiers of Biogeography, 15, e58651. https://doi.org/10.21425/F5FBG58651

Koch, P.L. & Barnosky, A.D. (2006) Late Quaternary extinctions: state of the debate. Annual Review of Ecology, Evolution, and Systematics, 37, 215-250. https://doi.org/10.1146/annurev.ecolsys.34.011802.132415

Lichstein, J.W., Simons, T.R., Shriner, S.A. & Franzreb, K.E. (2002) Spatial autocorrelation and autoregressive models in ecology. Ecological Monographs, 72, 445-463. https://doi.org/10.1890/0012-9615(2002)072[0445:SAAAMI]2.0.CO;2

Lovegrove, B.G. (2000) The zoogeography of mammalian basal metabolic rate. American Naturalist, 156, 201-219. https://doi.org/10.1086/303383

Lovegrove, B.G. (2003) The influence of climate on the basal metabolic rate of small mammals: a slow-fast metabolic continuum. Journal of Comparative Physiology B: Biochemical, Systemic, and Environmental Physiology, 173, 87-112. https://doi.org/10.1007/s00360-002-0309-5

Marquet, P.A., Quiñones, R.A., Abades, S., Labra, F., Tognelli, M., Arim, M. & Rivadeneira, M. (2005) Scaling and power-laws in ecological systems. Journal of Experimental Biology, 208, 1749-1769. https://doi.org/10.1242/jeb.01588

Martin, P.S. (1967) Prehistoric overkill. In: Pleistocene extinctions (ed. by P.S. Martin and H.E. Wright), pp. 75-120. Yale University Press, New Haven, CT.

Martin, P.S. (1984) Pleistocene overkill: the global model. In: Quaternary extinctions (ed. by P.S. Martin and R.G. Klein), pp. 354-403. University of Arizona Press, Tucson, AZ.

Maurer, B.A. (1996) Relating human population growth to the loss of biodiversity. Biodiversity Letters, 3, 1-5. https://doi.org/10.2307/2999702

McCabe, R.E. & McCabe, T.R. (1984) Of slings and arrows: an historical retrospective. In: White-tailed deer: ecology and management (ed. by L.K. Halls), pp. 19-72. Stackpole Books, Harrisburg, PA.

McNab, B.K. (1986) Food habits, energetics, and the reproduction of marsupials. Journal of Zoology, 208, 595-614. https://doi.org/10.1111/j.1469-7998.1986.tb01526.x

McNab, B.K. (1997) On the utility of uniformity in the definition of basal rate of metabolism. Physiological Zoology, 70, 718-720. https://doi.org/10.1086/515881

McNab, B.K. (2005) Uniformity in the basal metabolic rate of marsupials: its causes and consequences. Revista Chilena de Historia Natural, 78, 183-198. https://doi.org/10.4067/S0716-078X2005000200002

McNab, B.K. (2008) An analysis of the factors that influence the level and scaling of mammalian BMR. Comparative Biochemistry and Physiology Part A: Molecular and Integrative Physiology, 151, 5-28. https://doi.org/10.1016/j.cbpa.2008.05.008

Meltzer, D.J. (2020) Overkill, glacial history, and the extinction of North America's ice age megafauna. Proceedings of the National Academy of Sciences USA, 117, 28555-28563. https://doi.org/10.1073/pnas.2015032117

Mora, C. & Sale, P.F. (2011) Ongoing global biodiversity loss and the need to move beyond protected areas: a review of the technical and practical shortcomings of protected areas on land and sea. Marine Ecology Progress Series, 434, 251-266. https://doi.org/10.3354/meps09214

Nagy, K.A. (2005) Field metabolic rate and body size. Journal of Experimental Biology, 208, 1621-1625. https://doi.org/10.1242/jeb.01553

Naya, D.E., Spangenberg, L., Naya, H. & Bozinovic, F. (2013) How does evolutionary variation in basal metabolic rates arise? A statistical assessment and a mechanistic model. Evolution, 67, 1463-1476. https://doi.org/10.1111/evo.12042

Newbold, T., Hudson, L.N., Hill, S.L.L., et al. (2015) Global effects of land use on local terrestrial biodiversity. Nature, 520, 45-50. https://doi.org/10.1038/nature14324

Nordhaus, W.D. (2006) Geography and macroeconomics: new data and new findings. Proceedings of the National Academy of Sciences USA, 103, 3510-3517. https://doi.org/10.1073/pnas.0509842103

Nordhaus, W.D. & Chen, X. (2016) Data from: Global gridded geographically based economic data (G-Econ), version 4. NASA Socioeconomic Data and Applications Center (SEDAC), Palisades, NY.

Odum, E.P. (1968) Energy flow in ecosystems: a historical review. Integrative and Comparative Biology, 8, 11-18. https://doi.org/10.1093/icb/8.1.11

Parr, C.S., Wilson, N., Leary, P., et al. (2014) The encyclopedia of life v2: providing global access to knowledge about life on Earth. Biodiversity Data Journal, 2, e1079. https://doi.org/10.3897/BDJ.2.e1079

R Core Team (2022) R: A language and environment for statistical computing. R Foundation for Statistical Computing, Vienna, Austria.

Ripple, W.J., Wolf, C., Newsome, T.M., Betts, M.G., Ceballos, G., Courchamp, F., Hayward, M.W., Van Valkenburgh, B., Wallach, A.D. & Worm, B. (2019) Are we eating the world's megafauna to extinction? Conservation Letters, 12, e12627. https://doi.org/10.1111/conl.12627

Roberts, R.G., Flannery, T.F., Ayliffe, L.K., et al. (2001) New ages for the last Australian megafauna: continent-wide extinction about 46,000 years ago. Science, 292, 1888-1892. https://doi.org/10.1126/science.1060264

Rowan, J., Beaudrot, L., Franklin, J., Reed, K.E., Smail, I.E., Zamora, A. & Kamilar, J.M. (2020) Geographically divergent evolutionary and ecological legacies shape mammal biodiversity in the global tropics and subtropics. Proceedings of the National Academy of Sciences USA, 117, 1559-1565. https://doi.org/10.1073/pnas.1910489116

Rowcliffe, J.M., Field, J., Turvey, S.T. & Carbone, C. (2008) Estimating animal density using camera traps without the need for individual recognition. Journal of Applied Ecology, 45, 1228-1236. https://doi.org/10.1111/j.1365-2664.2008.01473.x

Saltré, F., Rodríguez-Rey, M., Brook, B.W., et al. (2016) Climate change not to blame for late Quaternary megafauna extinctions in Australia. Nature Communications, 7, 10511. https://doi.org/10.1038/ncomms10511

Sandom, C., Faurby, S., Sandel, B. & Svenning, J.C. (2014) Global late Quaternary megafauna extinctions linked to humans, not climate change. Proceedings of the Royal Society B: Biological Sciences, 281, 20133254. https://doi.org/10.1098/rspb.2013.3254

Savage, V.M., Allen, A.P., Brown, J.H., Gillooly, J.F., Herman, A.B., Woodruff, W.H. & West, G.B. (2007) Scaling of number, size, and metabolic rate of cells with body size in mammals. Proceedings of the National Academy of Sciences USA, 104, 4718-4723. https://doi.org/10.1073/pnas.0611235104

Schramski, J.R., Dell, A.I., Grady, J.M., Sibly, R.M. & Brown, J.H. (2015) Metabolic theory predicts whole-ecosystem properties. Proceedings of the National Academy of Sciences USA, 112, 2617-2622. https://doi.org/10.1073/pnas.1423502112

Smith, F.A., Elliott Smith, R.E., Lyons, S.K. & Payne, J.L. (2018) Body size downgrading of mammals over the late Quaternary. Science, 360, 310-313. https://doi.org/10.1126/science.aao5987

Smith, F.A., Elliott Smith, R.E., Lyons, S.K., Payne, J.L. & Villaseñor, A. (2019) The accelerating influence of humans on mammalian macroecological patterns over the late Quaternary. Quaternary Science Reviews, 211, 1-16. https://doi.org/10.1016/j.quascirev.2019.02.031

Smith, F.A., Hammond, J.I., Balk, M.A., Elliott, S.M., Lyons, S.K., Pardi, M.I., Tomé, C.P., Wagner, P.J. & Westover, M.L. (2016) Exploring the influence of ancient and historic megaherbivore extirpations on the global methane budget. Proceedings of the National Academy of Sciences USA, 113, 874-879. https://doi.org/10.1073/pnas.1502547112

Sollmann, R. (2018) A gentle introduction to camera-trap data analysis. African Journal of Ecology, 56, 740-749. https://doi.org/10.1111/aje.12557

Stiner, M.C. (2002) Carnivory, coevolution, and the geographic spread of the genus *Homo*. Journal of Archaeological Research, 10, 1-63. https://doi.org/10.1023/A:1014588307174

Thomas, M.L., Baker, L., Beattie, J.R. & Baker, A.M. (2020) Determining the efficacy of camera traps, live capture traps, and detection dogs for locating cryptic small mammal species. Ecology and Evolution, 10, 1054-1068. https://doi.org/10.1002/ece3.5972

Warton, D.I., Duursma, R.A., Falster, D.S. & Taskinen, S. (2012) smatr 3– an R package for estimation and inference about allometric lines. Methods in Ecology and Evolution, 3, 257-259. https://doi.org/10.1111/j.2041-210X.2011.00153.x

Wen, C., Zhang, A., Wang, X. & Quan, S. (2020) BeSS: an R package for best subset selection in linear, logistic and cox proportional hazards models. Journal of Statistical Software, 94, 1-24. https://doi.org/10.18637/jss.v094.i04

White, C.R. (2011) Allometric estimation of metabolic rates in animals. Comparative Biochemistry and Physiology Part A: Molecular & Integrative Physiology, 158, 346-357. https://doi.org/10.1016/j.cbpa.2010.10.004

White, C.R. & Seymour, R.S. (2004) Does basal metabolic rate contain a useful signal? Mammalian BMR allometry and correlations with a selection of physiological, ecological, and life-history variables. Physiological and Biochemical Zoology, 77, 929-941. https://doi.org/10.1086/425186

White, C.R. & Seymour, R.S. (2005) Allometric scaling of mammalian metabolism. Journal of Experimental Biology, 208, 1611-1619. https://doi.org/10.1242/jeb.01501

Wong, S.T., Belant, J.L., Sollmann, R., Mohamed, A., Niedballa, J., Mathai, J., Street, G.M. & Wilting, A. (2019) Influence of body mass, sociality, and movement behavior on improved detection probabilities when using a second camera trap. Global Ecology and Conservation, 20, e00791. https://doi.org/10.1016/j.gecco.2019.e00791

Yeo, I.K. & Johnson, R.A. (2000) A new family of power transformations to improve normality or symmetry. Biometrika, 87, 954-959. https://doi.org/10.1093/biomet/87.4.954

Submitted: 12 December 2023
First decision: 27 February 2024
Accepted: 4 March 2024

Edited by Janet Franklin

